Science and Engineering Connect, ISSN 3027-7914 (Online)
Vol. 47 No. 4 pp. 322-347 (2024)

Research Article

Utilization of Cassava Pulp from Starch Production Process and from Biogas System to Produce Value-Created Micro- and Nano-Cellulose

Chittaphone Banditvong, Navadol Laosiripojana,
The Joint Graduate School of Energy and Environment, King Mongkut's University of Technology Thonburi, Bangkok, Thailand
Suppanut Varongchayakul,
School of Bioresources and Technology, King Mongkut's University of Technology Thonburi, Bangkok, Thailand
Warinthorn Songkasiri*
National Center for Genetic Engineering and Biotechnology, Pathum Thani, Thailand
* Corresponding author E-mail: warinthorn@biotec.or.th

Received 27 May 2024; Revised 2 October 2024; Accepted 30 October 2024

Abstract

Background and Objective: Cassava pulp (CP) is a solid waste byproduct from the starch extraction process in the cassava industry, presenting significant environmental challenges such as foul odor and water contamination. In Thailand, the cassava industry has adopted the circularity concept to practice resource minimization, waste reduction, and value creation. Strategies have been developed to utilize CP for energy generation and low-value applications such as animal feed. Additionally, CP can be converted into biogas through anaerobic digestion. Another promising approach is the production of high-value products such as micro- and nano-cellulose. Micro-cellulose consists of micro-sized fibers isolated from plants, and can serve as a reinforcing material in the textile and pulp industries. Nano-cellulose, on the other hand, exhibits such properties as biodegradability and high surface area. These properties make micro-cellulose and nano-cellulose ideal for use as reinforcing polymers, food packaging, and pharmaceuticals. The present study aimed to produce micro-and nano-cellulose from CP obtained from (i) a starch production process and (ii) a biogas system (CP and CP_{biogas}, respectively) using acid hydrolysis.

Methodology: The study focused on the extraction of micro-cellulose and nano-cellulose from CP and CP_{biogas}. Starch was removed from CP using enzymatic treatment (**α**-amylase). Lignocellulosic fiber was then isolated using 0.7% (w/v) $NaClO_2$ and alkaline with 17.5% (w/v) NaOH to obtain micro-cellulose. Subsequently, the micro-cellulose was hydrolyzed with H_2SO_4 to produce nano-cellulose. The two-factor Central Composite Design (CCD) was utilized to optimize the design of the experiment. The two factors were H_2SO_4 concentration, ranging from 46-74% w/w and reaction time ranging from 48-132 min. In total, 11 experimental conditions were scheduled. The micro-cellulose and nano-cellulose obtained were characterized to determine their crystallinity indices using X-ray diffraction, their particle size using dynamic light scattering, and their morphology using scanning electron microscopy.
Main results: The study revealed that after the removal of starch by **α**-amylase, 87.5% of the starch was extracted from CP, while CP_{biogas} had all its starch removed. Following bleaching and alkaline treatment, a fibrous fraction with cellulose contents of 91% and 88% (CP and CP_{biogas} respectively) was obtained. The micro-cellulose extracted from CP and CP_{biogas} had average particle sizes of 104.9 μm and 106 μm and crystallinity indices of 68% and 70%, respectively. The optimal hydrolysis conditions for nano-cellulose extraction from CP and CP_{biogas} were 60% H_2SO_4 and 132-min reaction time. Nano-cellulose particles smaller than 100 nm comprised 10% and 12% of the total nano-cellulose yields from CP and CP_{biogas}, respectively, with an increase in crystallinity indices to 71% and 76%. Statistical analysis reveals that increasing the reaction time could result in a higher yield of nano-cellulose.
Conclusions: Micro-cellulose and nano-cellulose derived from CP and CP_{biogas} in exhibit promising characteristics, including crystallinity index of 71% and 76% for nano-cellulose obtained from CP and CP_{biogas}, respectively. Such characteristics demonstrate significant potential for innovative industrial applications in the paper, composite, and textile industries. In comparison, commercial nano-cellulose typically has a crystallinity index exceeding 80%; the nano-cellulose obtained in this study demonstrates crystallinity indices slightly below commercial standards. Utilizing solid wastes such as CP (CP and CP_{biogas}) to produce micro-cellulose and nano-cellulose addresses waste management challenges, while creating economic value from a previously underutilized byproduct.

Practical Application: The presented approach aligns with the principles of circular economy, where waste materials are repurposed into valuable resources, enhancing resource efficiency and sustainability. The study highlights the significant potential of converting CP waste into high-value cellulose products, contributing to the advancement of sustainable industrial practices and the development of innovative materials.

Keywords: Cassava Pulp, Chemical Treatment, Nanocellulose, Starch Waste, Sustainable Material

Introduction

Thailand has implemented the circularity concept for the cassava starch industry. Circularity is defined as resource minimization, waste reduction, and value creation. Cassava, or tapioca, is an important commodity crop cultivated around the world. The traditional cassava value chain includes cultivation of cassava roots, transformation of roots into chips, pellets, and native starch. Native starch is then modified physically, chemically, or biologically with various applicable properties. Some factories utilize roots to produce bioethanol. The production of native starch has generated wastewater and solid wastes such as cassava pulp (CP), peel, and rhizomes. To produce 1 ton of cassava starch, approximately 4.4 tons of cassava roots is used. This process generates solid wastes consisting of 2.5 tons of CP, 600 kg of rhizomes, 170 kg of sand, and 100 kg of cassava peels [1].

In 2021, Thailand's cassava starch production was 10.8 million tons, and the generated CP was 27 million tons [2]. CP is generated during the extraction of starch from cassava roots. The composition of CP directly from the starch production process has a moisture content of 80% (weight basis), a high starch content of 60-75%, 4-15% cellulose, 4-5% hemicellulose, and 1-3% lignin (dry basis) [3]. This waste presents a significant challenge in terms of disposal due to its high moisture content and limited storage life. However, the cassava starch industry has developed various strategies to address this issue, primarily by focusing on the utilization of CP for energy generation or low-value applications such as animal feed. Although CP has limited nutritional value compared to fresh cassava roots or starch, it can still serve as a supplementary feed ingredient for livestock. By processing and enriching CP with other feed components, such as protein sources or mineral

supplements, it can contribute to the nutritional requirements of animals, thus providing a low-cost alternative feed source for farmers. While this application may not maximize the value of CP, it helps reduce waste and supports sustainable agricultural practices.

Another utilization pathway for CP is the conversion of CP into biogas through anaerobic digestion, offering a dual benefit of waste management and energy generation. Anaerobic microorganisms break down organic materials, such as starch, cellulose, and hemicellulose, in the absence of oxygen, producing biogas. The primary components of biogas are methane (CH_4) and carbon dioxide (CO_2), with trace amounts of other gases. Methanogenic archaea play a central role in this process, leading to the production of methane, a valuable renewable energy resource for applications such as heat and electricity generation [4].

Alternative utilization to create value-added production from waste is still needed for the cassava starch industry, and one example is the extraction of micro- and nano-cellulose from CP. In recent years, cellulose has emerged as a key player in the quest for eco-friendly materials, renewable energy sources, and biotechnological advancements. Its remarkable properties, including biodegradability, renewable sourcing, and versatile applicability, position cellulose as a cornerstone in the transition towards a more sustainable future [5].

Cellulose is a complex carbohydrate consisting of linear chains of β-glucose molecules linked together by β (1-4) glycosidic bonds. Cellulose is a fundamental polysaccharide found in the cell walls of plants, algae, and certain bacteria [6]. Micro- and nano-cellulose are derived from cellulose, a natural polymer abundant in plants, through controlled chemical or mechanical treatments that break down cellulose fibers into smaller crystalline particles. Microcrystalline cellulose (MCC) typically refers to particles on the micrometer scale, while nanocrystalline cellulose (NCC) refers to even smaller particles, usually in the nanometre range. MCC and NCC exhibit remarkable properties that make them attractive for a wide range of applications. Their high aspect ratio, large surface area, and biodegradability render them suitable for use in composite materials, biomedical devices, and functional coatings [7]. The production of MCC and NCC involves several methods, including acid hydrolysis, high-pressure homogenization, and enzymatic hydrolysis. These techniques aim to break down cellulose fibers into smaller crystalline particles while preserving their inherent properties [8]. Each method offers unique advantages in terms of scalability, cost-effectiveness, and control over particle size and morphology. NCC can be produced through enzymatic hydrolysis. In previous studies, cotton fibers pretreated with dimethyl sulfoxide (DMSO),

NaOH, and ultrasonic waves, followed by hydrolysis with Cellulases (*T. viride*), produced nanosized strip-like (10 to 40 nm × 70 to 280 nm) and granular NCC (20 nm or 6 nm) with a maximum yield of 32.4% [8]. Similarly, enzymatic hydrolysis of cotton fibers using cellulases (*A. niger*) resulted in ribbon-like NCC at lower enzyme concentrations, while higher concentrations led to granular NCC (enzyme loading of 10-300 μ/mL) [9]. Bamboo fibers hydrolyzed with cellulase (*T. reesei*) produced rod-like NCC, with a zeta potential four times lower than acid-hydrolyzed NCC, indicating distinct surface properties [10]. However, the main drawback of enzymatic hydrolysis is the long reaction time, typically 48 to 72 hours. [11]. Another method for cellulose hydrolysis employs strong acid, typically H_2SO_4. This process selectively removes the amorphous regions of cellulose, resulting in a higher proportion of crystalline regions of cellulose. Acid hydrolysis offers higher yields, approximately at 90% based on initial cellulose, with short reaction times of 2-6 h [12]. The utilization of waste CP and CP_{biogas} to produce MCC and NCC presents an innovative approach towards sustainable waste management and resource utilization. The study on cellulose isolation at the micro- and nanoscale requires further research, particularly regarding the effects of acid concentration and reaction time on hydrolysis. To date, no comparative research has been conducted on the isolation of MCC and NCC from CP and CP_{biogas} for potential industrial-scale production. Thus, this study aimed to investigate the extraction process of MCC and NCC from CP and CP_{biogas}, based on the method described by Travalini et al. 2018 [13]. The expected outcome was to produce MCC and NCC with low production costs, environmentally friendly procedures, and low energy consumption, while achieving high crystallinity, and high yield.

Materials and Methods

Extraction of MCC and NCC was performed using CP and CP_{biogas} as raw materials The extraction process consisted of three main steps: (1) starch removal by enzymatic treatment (α-amylase), (2) hemicellulose and lignin removal using 0.7% (w/v) $NaClO_2$ and 17.5% (w/v) NaOH, and (3) acid hydrolysis using H_2SO_4 at differing concentrations and varying reaction times. The resulting suspension was freeze-dried prior to characterization of MCC and NCC (Figure 1).

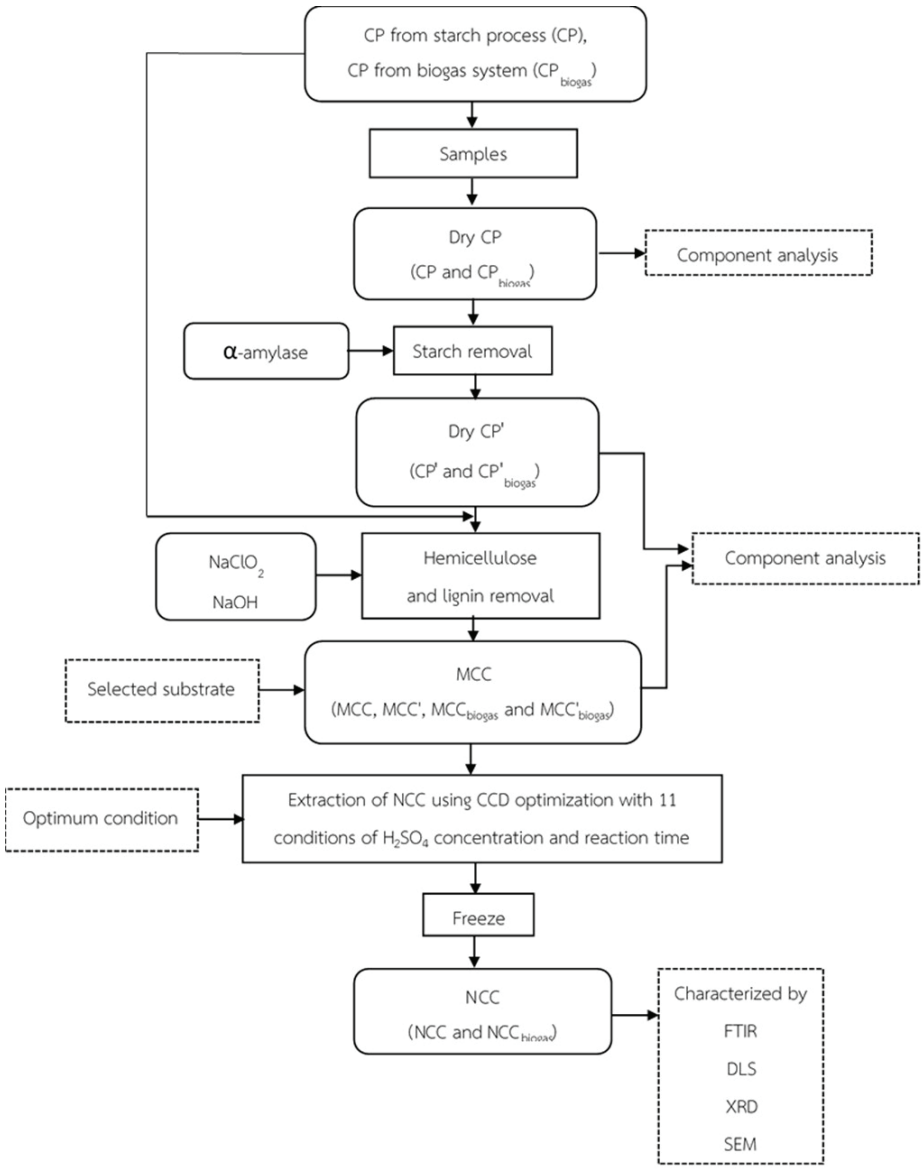

Figure 1 Overview of Experimental Program

Materials

Fresh CP was collected from the CP extraction unit, while CP_{biogas} was collected from the residual solids of the anaerobic digestion system, which utilizes CP for biogas production. Both substrates were obtained from a starch factory in the northeastern region of Thailand. The samples were stored in a freezer at -20°C to preserve its integrity for the experiment.

The chemical composition, including moisture content, total solid (TS), volatile solid (VS), and ash content of both CP and CP_{biogas} was determined using a standard AOAC method [14]. The starch content was analyzed using an enzymatic method [15].

Cellulose, hemicellulose, and lignin content were determined from neutral detergent fiber (NDF), acid detergent fiber (ADF), and acid detergent lignin (ADL) using the Van Soest and McQueen & Nicholson method [16]. All components were reported on a % dry basis.

Starch Removal

Fresh CP and CP_{biogas} were treated with **α**-amylase (Bacillus licheniformis) from Power Tech Chemical Industry Co., Ltd, (PTCI), Thailand, which has a specific activity of 3,000 U/mL. Each substrate was mixed at a specific ratio of 1 kg fresh sample to 5 L water to 5 mL **α**-amylase. Then, the mixture was boiled at 95-100°C for 2 h. Samples were tested using the iodine method to monitor the starch content. Later, the solution was washed to remove any residual starch and dried at 55°C. The dried sample was ground and sifted through a sieve with a size of 500 µm for further use. This pretreatment aimed to remove the residual starch entrapped in the substrate to obtain mainly the fiber component. Fresh CP and CP_{biogas} after the starch removal process are referred to as CP' and CP'_{biogas}, respectively.

Microcrystalline Cellulose (MCC) Extraction

The CP, CP', CP_{biogas} and CP'_{biogas} were firstly bleached using the method described by Mandal and Chakrabarty 2011 [17]. The 0.7% (w/v) $NaClO_2$ solution was added to dry CP, CP', CP_{biogas} and CP'_{biogas} at a fiber-to-solution ratio of 1:50 (w/v) and the pH was adjusted to 4 with a 5% (v/v) CH_3COOH. This mixture was then boiled for 5 h for hemicellulose removal. Subsequently, the material was filtered using a vacuum pump, washed with distilled water, and boiled in 50 mL of 5% (w/v) Na_2SO_3 solution for 5 h for lignin removal. This procedure was repeated multiple times to maximize lignin removal.

The next extraction step was alkaline treatment where the CP, CP', CP_{biogas} and CP'_{biogas} were boiled in 50 mL of 17.5% (w/v) NaOH solution for 5 h. The samples were then filtered and washed with distilled water until reaching neutral pH. The samples were dried at 55°C for 12 h and then suspended in 50 mL of dimethyl sulfoxide (DMSO) at 80°C for 3 h. The product was filtered using a vacuum pump, washed with distilled water, and dried at 55°C for 12 h. Finally, the resulting MCC, MCC', MCC_{biogas} and MCC'_{biogas} obtained were ground and sieved (250 µm). Following the MCC extraction, the sample yield was calculated using Eq (1).

$$\% \text{ Yield} = \frac{B}{A} \times 100 \quad \textbf{(Eq. 1)}$$

Where A is the weight of the sample before treatment (g dry sample)
B is the weight of the sample after treatment (g dry sample)

Nanocrystalline Cellulose (NCC) Extraction Using Acid Hydrolysis

The extraction of NCC from MCC' and MCC_{biogas} was performed using H_2SO_4 hydrolysis. The optimization of reaction conditions for NCC extraction from MCC' and MCC_{biogas} focused on H_2SO_4 concentration and reaction time. The central composite design (CCD) was employed to design the optimization conditions where the two factors were H_2SO_4 concentrations ranging from 46-74% w/w and reaction time ranging from 48-132 min. A total of 11 experiments incorporating 4 axial points, 4 quadratic points, and 3 center points runs were designed as shown in Table 1.

Minitab 18.1 software was used for statistical analysis, facilitating the identification of optimal conditions, based on the application of Eq (2):

$$Y = \beta_0+\beta_1A+\beta_2B+\beta_3A^2+\beta_4B^2+\beta_5AB \quad \textbf{(Eq. 2)}$$

where Y is the response (total amount of NCC yield), βi is the regression coefficients for each variable, A is the concentration (%), and B is the reaction time (min).

Table 1 Experimental Design of NCC Extraction

Experiment No.	Code Value		Actual Value	
	H_2S0_4 (A)	Time (B)	H_2SO_4 (%w/w)	Time (min)
1	-1	-1	50	60
2	-1	1	50	120
3	1	-1	70	60
4	1	1	70	120
5	-1.414	0	46	90
6	1.414	0	74	90

Table 1 Experimental Design of NCC Extraction (Continued)

Experiment No.	Code Value		Actual Value	
	H_2S0_4 (A)	Time (B)	H_2SO_4 (%w/w)	Time (min)
7	0	-1.414	60	48
8	0	1.414	60	133
9	0	0	60	90
10	0	0	60	90
11	0	0	60	90

Initially, 1.5 g of MCC' and MCC_{biogas} (dry basis) were mixed with H_2SO_4 and incubated at 45°C, where the H_2SO_4 concentration and reaction time were based on the experimental conditions. After hydrolysis, the sample was washed with distilled water and centrifuged at 4,000 rpm for 10 min; this process was repeated until the sample reached neutral pH. Then, the suspension was dialyzed against distilled water for 12 h using a regenerated cellulose membrane (14,000 Da, Sigma Aldrich, USA). Subsequently, the samples were filtered using filter paper (Whatman GF/C with 1.2 µm pore size) to obtain NCC with sizes of less than 1.2 µm. The clear hydrolysate obtained after filtering was used to analyze the size of NCC, which was performed using Dynamic Light Scattering (DLS, Malvern Zetasizer, UK). The amount of NCC and NCC_{biogas} with sizes less than 100 nm ($NCC_{<100nm}$ and $NCC_{biogas<100nm)}$ was calculated using Eq. (3):

$$\text{Yield of NCC} = \frac{D}{C} \quad \textbf{(Eq. 3)}$$

Where C is the weight of the sample before H_2SO_4 hydrolysis (g dry sample)

D is the weight of the sample with particle sizes <100nm after H_2SO_4 hydrolysis (g dry sample)

NCC Preservation Using Freeze Drying

The samples were first frozen at -80°C and then subjected to freeze-drying using a Freeze Dryer (Economic-gold-sim model, CELLULAR SCIENCE LLC, USA) to preserve the morphology and properties of the nanocellulose for subsequent analyses.

NCC Characterization

Fourier Transform Infrared Spectroscopy

Fourier-Transform Infrared (FTIR) spectroscopy (PerkinElmer, SPECTRUM ONE, Canada) was employed to examine the spectral characteristics of the sample. The FTIR spectra were recorded using a high-resolution spectrophotometer over a broad wavenumber range from 4000 to 450 cm^{-1}. First, samples were dried to remove moisture. Subsequently, the dried samples were finely ground to a consistent particle size. The ground materials were pelletized with high-purity potassium bromide (KBr). This method ensured that the samples were uniformly distributed and effectively analyzed in the FTIR spectroscopic analysis, enabling a deeper understanding of the structural and chemical properties.

X-ray Diffaction Analysis

X-ray diffraction (XRD) was used to analyze the crystallinity index of materials. A sample was irradiated with X-rays generated from a copper anode (CuKα radiation, λ = 1.5406 Å) at a power level of 40 kV and a current of 30 mA. The data acquisition was performed at a scan rate of 0.5° per minute, covering a range of 2θ angles from 10° to 30° [18]. The crystallinity index was calculated according to Eq. (4):

$$CrI = \left(1 - \frac{I_{(am)}}{I_{(200)}}\right) \times 100 \quad \textbf{(Eq. 4)}$$

where: $I_{(am)}$ is the diffraction intensity of the amorphous material.

$I_{(200)}$ is the main diffraction peak intensity, representing the crystalline and amorphous material.

Scanning Electron Microscopy

The morphological analysis was conducted using a scanning electron microscope, SEM (JSM-7800F PRIME Schottky Field Emission Scanning Electron Microscope, Japan). The samples were first coated with a thin layer of gold and then examined under accelerated electrons with an energy of 10 kV.

Results and Discussion

Characterization of CP and CP_{biogas}

The CP and CP_{biogas} samples were obtained from the cassava starch factory in the northeastern region of Thailand. For the compositional analysis, the conventional CP exhibited a moisture content of 81.8% wet basis, indicating a TS content of 18.2%. Similarly, the CP_{biogas} demonstrated a moisture content of 85.6% wet basis, corresponding to a TS content of 14.4%. This variation in moisture content between the two sources is a noteworthy consideration in subsequent analyses.

The CP contained a high VS of 97.9% dry basis, while the CP_{biogas} had a VS of 90.2% dry basis. This high VS content suggests that the CP is predominantly composed of organic matter. The VS content of CP_{biogas} was slightly lower when compared to CP. This difference suggests that the biogas production process may have partially degraded the organic matter present in the cassava pulp. However, CP_{biogas} still retains a substantial amount of organic matter. The ash content of CP was 2.1%. Ash content represents the inorganic mineral residue left after the complete combustion of organic matter. A low ash content of CP indicates minimal inorganic impurities, making CP a desirable raw material for producing MCC and NCC. In contrast, CP_{biogas} exhibited a higher ash content at 9.8%. This increase in ash content could be attributed to mineral accumulation during the biogas production process.

The CP consisted predominantly of starch, followed by cellulose, hemicellulose, and lignin. The percentages were 46.5% starch, 19.8% cellulose, 5.8% hemicellulose, and 3.3% lignin on a dry basis (Table 2). The composition of CP in this study shows variations compared to previous studies, which found cellulose content ranging from 4-15%, hemicellulose from 4-5%, and lignin from 1-2% [19-20]. However, the starch content appeared lower in this study. These variations could be attributed to differences in processing methods and starch extraction efficiency in different studies. CP_{biogas} exhibited a significant reduction in starch content, indicating utilization during the anaerobic digestion process for biogas production. The remaining components were mainly fibrous materials, consisting of 53.0% cellulose, 11.1% hemicellulose, and 9.9% lignin on a dry basis. The cellulose and lignin contents also increased on a dry basis, which could be attributed to the properties of lignocellulosic residues after starch removal.

Composition of CP and CP_{biogas} after Starch Extraction (CP' and CP'_{biogas})

Table 2 shows the composition of CP' and CP'_{biogas}. The CP' exhibited an increased proportion of fibers due to the reduction in starch content. The yield of CP' was 48.6% based on the initial dry weight of CP. The starch content decreased from 46.5% to 5.8%, indicating an 87.5% removal efficiency. For CP'_{biogas}, starch was completely eliminated, resulting in a composition of 16.2% cellulose, 6.0% hemicellulose, and 6.2% lignin.

Table 2 Chemical Compositions of CP, CP', CP_{biogas} and CP'_{biogas}

Sample	Composition (%Dry Basis Based on Initial Weight)				
	Solid remaining	Starch	Cellulose	Hemi - cellulose	Lignin
CP	100.0±0.0	46.5±1.0	19.8±0.3	5.8±0.2	3.3±0.3
CP'	48.6±0.4	5.8±0.2	16.2±1.9	6.0±1.1	6.2±2.2
CP_{biogas}	100.0±0.0	5.2±0.1	53.0 ±0.5	11.1±1.0	9.9 ±0.3
CP'_{biogas}	83.4±0.5	0	44.0±2.4	9.0 ±0.1	18.5±2.3

Extraction of MCC, MCC', MCC_{biogas} and MCC'_{biogas} Fibers

After the starch removal process, the yield of MCC was 7.2% based on the dry CP. The MCC consisted of 92.5% cellulose and 3.4% hemicellulose, while the lignin and starch were completely removed (Table 3). The yield of MCC' was 13.5% based on dry CP'. The composition of MCC' was 1.4% starch, 91.0% cellulose, and 3.4% hemicellulose, while lignin was completely removed (Table 3).

The yield of MCC_{biogas} was 13% based on the initial dry weight of CP_{biogas}. With a composition of 88.5% cellulose and 4.1% hemicellulose, while the lignin and starch were completely removed. The yield of MCC'_{biogas} was 19.1% based on dry CP'_{biogas}, comprising 85.6% cellulose and 3.4% hemicellulose, while the lignin and starch were completely removed.

The MCC yields from different substrates after the bleaching process varied, ranging from 7.2% to 19.1% based on the initial composition of the respective initial substrates. This variation suggests that the initial composition of the substrates or differences in the bleaching process efficiency may influence the yield of purified MCC. The complete removal of lignin

and starch during the bleaching process indicates its effectiveness in selectively removing non-cellulosic components from the raw material. The use of $NaClO_2$ for lignin removal and NaOH treatment for hemicellulose degradation proved to be effective, resulting in a purified MCC product with minimal hemicellulose content. This effect is due to 1) $NaClO_2$ binding to lignin bonds in the form of lignin chloride compounds or complexes to remove lignin, and 2) NaOH (alkali) treatment degrading the glycosidic bonds of the xylose, mannose, and glucose constituents of the hemicellulose structure and cleaving the ester bonds between hemicellulose and lignin.

Figure 2 presents the SEM images of (a) CP, (b) MCC', (c) CP_{biogas} and (d) MCC_{biogas}, revealing the increased whiteness of the fiber after the bleaching procedure. Based on the composition of the four substrates, the MCC' and MCC_{biogas} provided a higher yield and hence these substrates were selected for NCC extraction in the next step.

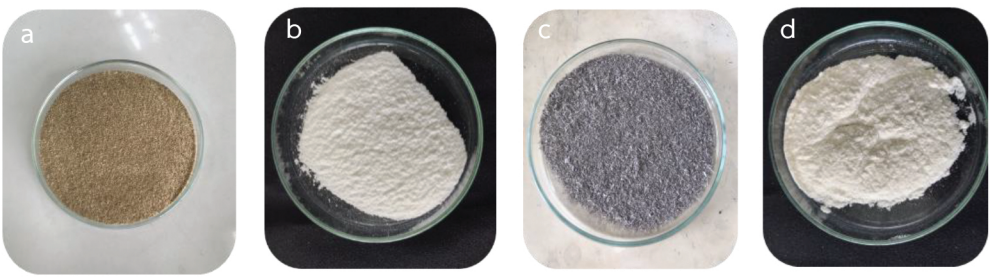

Figure 2 Images of (a) CP, (b) MCC', (c) CP_{biogas} and (d) MCC_{biogas}

Table 3 Compositions of Materials Before and After Hemicellulose and Lignin Removal

Sample	Component % Dry Basis						
	VS	Starch	Cellulose	Hemi - cellulose	Lignin	Ash	Other
CP'	96.0±0.2	11.9±0.2	33.5±1.9	12.7±1.1	14.0±2.2	4.1±0.0	-
MCC	99.8±0.0	0	92.5±0.5	3.4±0.5	0	0.2±0.0	-
MCC'	99.8±0.1	1.4±0.2	91.0±0.9	3.4±0.6	0	0.2±0.1	-
CP'_{biogas}	91.9±0.7	0	43.2±2.4	9.3±0.1	22.9±2.3	8.1±0.7	-
MCC_{biogas}	95.6±0.3	0	88.5±2.2	4.1±0.2	0	4.4±0.3	-
MCC'_{biogas}	91.2±1.3	0	85.6±0.8	3.4±0.8	0	8.8±1.3	-

Extraction Using Acid Hydrolysis

The residual total solids (TS) of NCC and NCC_{biogas} after acid hydrolysis at different H_2SO_4 concentrations and reaction times were summarized in Table 4. The highest residual TS level of NCC and NCC_{biogas} were found when hydrolyzed at a H_2SO_4 concentration of 46% for 90 min (95.6% from NCC and 88.0% from NCC_{biogas}), although 50% H_2SO_4 for 60 and 120 min also yielded similar results (84.7% and 79.2% from NCC; 82.8% and 79.9% from NCC_{biogas}), while 60% H_2SO_4 for 48, 90, and 132 min showed minimal variation (74.0%, 67.2% and 65.9% from NCC; 74.3%, 61.3% and 57.9% from NCC_{biogas}). In contrast, treatment with 70% H_2SO_4 for 60 and 120 min demonstrated a completely decreased TS (completely decreased of both conditions 0.3%, 0.3% from NCC and 9.4%, 9.8% from NCC_{biogas}), and the highest tested H_2SO_4 concentration of 74% for 90 min resulted in TS (13.2% from NCC and 24.7% from NCC_{biogas}). To conclude, the highest TS of NCC and NCC_{biogas} was obtained at 46% H_2SO_4, followed by 50%, 60%, 70%, and 74% H_2SO_4. In addition, TS content after treatment with 70% and 74% H_2SO_4 yielded negligible. Therefore, H_2SO_4 concentrations of 70% and 74% were unsuitable for NCC extraction.

As a strong mineral acid, H_2SO_4 has gained prominence in the realm of NCC extraction due to its unique and effective role in depolymerizing cellulose fibers. This lies in its ability to catalyze the hydrolysis of cellulose, leading to the production of NCC with remarkable properties. Its role as a catalyst in the hydrolysis process is instrumental in breaking down cellulose fibers into nanoscale dimensions, a crucial step in NCC production. In addition, too low a H_2SO_4 concentration may result in inefficient depolymerization of cellulose and so a reduced NCC yield. Conversely, an excessively high H_2SO_4 concentration (70% and 74%) may result in the degradation of NCC, compromising its quality.

Additionally, this study also determined the yield of NCC with a size smaller than 100 nm ($NCC_{<100}$) under various experimental conditions. The highest $NCC_{<100}$ and $NCC_{biogas<100}$ yields were obtained with 60% H_2SO_4 for 132 min at 0.066g and 0.064g, respectively, followed by 60% H_2SO_4 for 90 min (0.020g from NCC and 0.033g from NCC_{biogas}), 74% H_2SO_4 for 90 min (0.020g from NCC and 0.029g from NCC_{biogas}) and 50% H_2SO_4 yielded range from 0.002g-0.014g. These results indicate that both H_2SO_4 concentration and reaction time significantly influenced NCC yield and size distribution.

Table 4 Residual Total Solids (TS) and Yield of $NCC_{<100nm}$ and $NCC_{biogas<100nm}$ after Acid Hydrolysis Under Various Experimental Conditions

Experiment No.	H_2SO_4 (%w/w)	Time (min)	TS of NCC after H_2SO_4 Hydrolysis (%Dry Basis Based on Initial Weight)	TS of NCC biogas after H_2SO_4 Hydrolysis (%Dry Basis Based on Initial Weight)	$NCC_{<100nm}$ (g/g Dry Sample)	$NCC_{biogas<100nm}$ (g/g Dry Sample)
1	50	60	84.7	82.8	0.014	0.000
2	50	120	79.2	79.9	0.002	0.000
3	70	60	0.3	9.4	0.000	0.000
4	70	120	0.3	9.8	0.000	0.000
5	46	90	95.6	88.0	0.000	0.000
6	74	90	13.2	24.7	0.029	0.020
7	60	48	74.0	74.3	0.004	0.003
8	60	132	65.9	57.9	0.066	0.064
9	60	90	64.1	61.6	0.019	0.032
10	60	90	67.6	63.5	0.025	0.033
11	60	90	65.9	58.7	0.018	0.034

Optimization of NCC and NCC_{biogas}

The yields of NCC and NCC_{biogas} were used as a response in statistical analysis. Before conducting the analysis of variance (ANOVA), the normality of data was assessed. The results indicated that the NCC and NCC_{biogas} fitted a normal distribution. Subsequently, ANOVA was employed to analyze the response surface quadratic model. This analysis further explored relationships between factors to optimize the NCC extraction process as shown in Tables 5 and 6.

The coefficient analysis was determined using a t-test and p-value. The coefficient analysis of NCC (Eq. 5) revealed that the concentration and reaction time had a positive effect (+0.00059) on the NCC yield, where increasing the H_2SO_4 concentration and reaction time increased the NCC yield. For the quadratic factors, the acid concentration and reaction time had a negative coefficient (-0.00707,-0.000039, respectively). The coefficient of interaction was negative, which means the combination of these two factors tended to decrease even though the individual factor increased the amount of NCC. On the other hand, increasing only the reaction time would give a higher NCC yield. The coefficient analysis of NCC_{biogas} (Eq. 6) revealed that the concentration and reaction time had a negative effect (-0.00090), which means the NCC yield increased until it reached a specific value and then started to decrease, especially for increasing acid concentrations. For the quadratic factors, the acid concentration and reaction time had negative coefficients (-0.00680,-0.000186, respectively), similar to those for NCC.

$$NCC = -23.4 + 0.802\,Conc - 0.018\,Time - 0.00707\,Conc*Conc - 0.000039\,Time*Time + 0.00059\,Conc*Time \quad \textbf{(Eq. 5)}$$

$$NCC_{biogas} = -33.8 + 0.932\,Conc + 0.1041\,Time - 0.00680\,Conc*Conc - 0.000186\,Time*Time - 0.00090\,Conc*Time \quad \textbf{(Eq. 6)}$$

For optimization, the maximum yield for NCC and NCC_{biogas} were determined to obtain the optimum conditions, which were found to be at 62% H_2SO_4 for 132 min (Figure 3a) and 59% H_2SO_4 for 132 min (Figure 3b), respectively. However, the predicted values were not majorly different from the experimental one at 60% H_2SO_4 for 132 min, and hence this study used the experimental condition for NCC extraction in the next step. Nevertheless, this optimization may not have resulted in the optimum condition due to the p-values for the lack of fit of $NCC_{<100nm}$ and $NCC_{biogas<100nm}$ being 0.004 and 0.000, respectively. The p-values were lower than 0.05 suggesting that the model did not entirely fit the data and required refinement or that other influencing factors were omitted. In addition, the mathematical model of $NCC_{<100nm}$ and $NCC_{biogas<100nm}$ with R-squared values of 32% and 67% and adjusted R-squared values of 0% and 34%, respectively. These low R-squared values indicate that the models explain only a small portion of the variability in the data, further supporting the need for model refinement.

Table 5 Analysis of Variance of NCC

Source	DF	Adj SS	Adj MS	F-Value	P-Value
Model	5	3.9843	0.79686	0.47	0.784
Linear	2	0.8520	0.42600	0.25	0.785
Conc	1	0.0475	0.04749	0.03	0.873
Time	1	0.8045	0.80452	0.48	0.520
Square	2	3.0049	1.50246	0.89	0.465
Conc*Conc	1	2.8204	2.82038	1.68	0.252
Time*Time	1	0.0070	0.00695	0.00	0.951
2-Way Interaction	1	0.1274	0.12737	0.08	0.794
Conc*Time	1	0.1274	0.12737	0.08	0.794
Error	5	8.3943	1.67886		
Lack -of-Fit	3	8.3702	2.79006	231.15	0.004
Pure Error	2	0.0241	0.01207		
Total	10	12.3786			

Table 6 Analysis of Variance of NCC_{biogas}

Source	DF	Adj SS	Adj MS	F-Value	P-Value
Model	5	5.75224	1.15045	2.01	0.231
Linear	2	2.83785	1.41893	2.48	0.179
Conc	1	0.91686	0.91686	1.60	0.262
Time	1	1.92100	1.92100	3.35	0.127
Square	2	2.62072	1.31036	2.29	0.197
Conc*Conc	1	2.61427	2.61427	4.56	0.086
Time*Time	1	0.15903	0.15903	0.28	0.621
2-Way Interaction	1	0.29367	0.29367	0.51	0.506
Conc*Time	1	0.29367	0.29367	0.51	0.506
Error	5	2.86388	0.57278		
Lack -of-Fit	3	2.86376	0.95459	16474.02	0.000
Pure Error	2	0.00012	0.00006		
Total	10	8.61612			

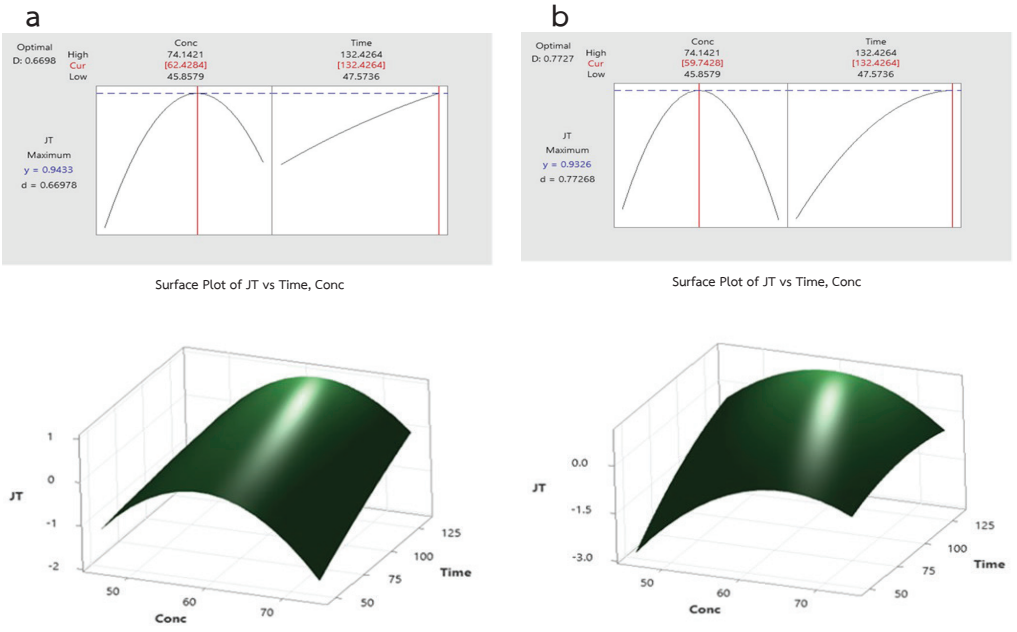

Figure 3 a). 3D Response Surface Plots between H_2SO_4 Concentration and Reaction Time on NCC Yield

b). 3D Response Surface Plots between H_2SO_4 Concentration and Reaction Time on NCC_{biogas} Yield

Crystallinity Index

The crystalline structure of the obtained MCC and NCC was investigated using XRD analysis. Cellulose has both crystalline and amorphous regions. On removing the non-cellulosic constituents from the fibers by chemical treatment, the degree of crystallinity of the fiber was changed [21]. From Figure 4, we can note that all the diffractograms showed a peak at 15° and 21.92°. The crystallinity of CP, MCC, MCC', and NCC was found to be 22%, 68%, 68%, and 71%, respectively, while that for CP_{biogas}, MCC_{biogas}, MCC'_{biogas}, and NCC_{biogas} was 43%, 70%, 73%, and 76%, respectively (Table 7). The observed increase in crystallinity after bleaching can be attributed to the removal of non-cellulosic components and impurities during the bleaching process. Crystallinity refers to the proportion of crystalline regions within the cellulose structure compared to the total cellulose content. These impurities can disrupt the orderly arrangement of cellulose chains, leading to a lower crystallinity. The removal of these impurities through bleaching enhances the purity of the cellulose, contributing to the observed increase in crystallinity.

The comparison of the crystallinity index between NCC and NCC_{biogas}, revealed values of 71% and 76%, respectively. A higher crystallinity index often indicates a greater proportion of well-organized crystalline regions within the cellulose structure. In the context of NCC production, a higher crystallinity index is generally desirable as it is associated with enhanced mechanical strength, thermal stability, and other favorable properties. In this case, the NCC_{biogas} exhibited a higher crystallinity index (76%) compared to NCC (71%), suggesting that NCC_{biogas} possessed a more ordered and crystalline structure. This increase in crystallinity may be attributed to specific factors involved in the biogas production process, such as the microbial breakdown of organic matter, which could result in cellulose with a higher degree of structural organization. The higher crystallinity index in NCC_{biogas} could potentially translate into improved performance in various applications, particularly in industries where NCC is utilized for its mechanical and thermal properties. However, it's essential to consider other factors, such as the overall yield, purity, and specific application requirements, when determining the most suitable source for nanocellulose production.

Thus, to confirm the effect of hemicellulose and lignin removal, the CP, MCC, MCC', and NCC; CP_{biogas}, MCC_{biogas}, MCC'_{biogas} and NCC_{biogas} samples were analyzed by FTIR spectroscopy (Figure 5). Both CP and CP_{biogas} showed peaks at wavenumbers around 1700-1730 cm^{-1}, ascribed to the acetyl and ester groups of the uronic ester in pectin, hemicellulose structure, or the ester bond of the ferulic acid and p-coumaric acid of lignin [19]. Additionally, the presence of lignin is related to the evident peak at 1245 cm^{-1} that is ascribed to the C-H, O-H, or CH_2 bending of the aryl group of lignin [22]. Whereas MCC, MCC', NCC, MCC_{biogas}, MCC'_{biogas} and NCC_{biogas} did not show absorbance in this range, meaning the hemicellulose and lignin had been removed. The peaks of β-glycosidic bonds between the glucose groups of cellulose at wavenumbers of 890-900 cm^{-1} were evident due to the removal of hemicellulose and lignin that results in a higher cellulose purity.

Table 7 Crystallinity Index of Cellulose Fibers

Samples	CrI (%)	Samples	CrI (%)
CP	22	CP_{biogas}	43
MCC	68	MCC_{biogas}	70
MCC'	68	MCC'_{biogas}	73
NCC	71	NCC_{biogas}	76

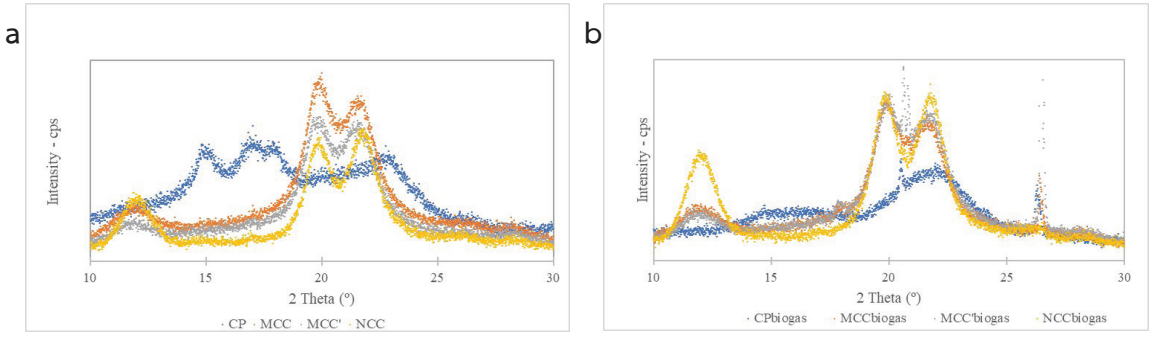

Figure 4 Representative XRD Spectra of (a) CP, MCC, MCC', and NCC; and (b) CP_{biogas}, MCC_{biogas}, MCC'_{biogas}, and NCC_{bioga}

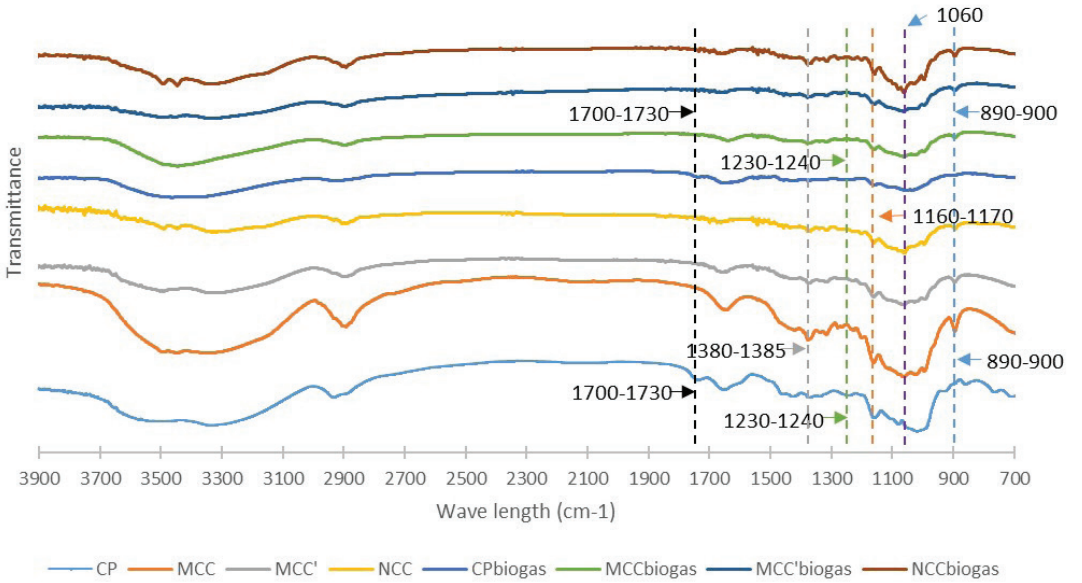

Figure 5 Representative FTIR Spectra of CP, MCC, MCC', NCC, CP_{biogas}, MCC_{biogas}, MCC'_{biogas} and NCC_{biogas}

Scanning Electron Microscopy

Figure 6 shows SEM images to reveal the morphology of the CP, CP', MCC', NCC, CP_{biogas}, CP'_{biogas}, MCC'_{biogas}, and NCC_{biogas}. The CP had rough surfaces attributable to the presence of fibers and starch granule constituents (Figure 6a). After starch removal, the surface of CP' exhibited a greater smoothness compared to CP (Figure 6b), consistent with the chemical composition analysis that showed a decreased starch content. The morphology of CP_{biogas} featured dense surfaces with thick-walled fiber cells interconnected with pith. The fibers exhibited parallel stripes with fewer starch granules (Figure 6e) due to digestion in the biogas system and was like CP_{biogas} after the starch removal (Figure 6f). Figures 6c and 6g show MCC, depicting the weakened networks from hemicellulose and lignin removal during the treatment. Figures 6d and 6h show the NCC extracted after H_2SO_4 hydrolysis, which typically cleaves the amorphous regions of microfibrils transversely in cellulose fibers, resulting in a significant reduction in the fiber diameter from the micron to nanometer scale [23]. However, due to the low yield of $NCC_{<100nm}$ and $NCC_{biogas<100nm}$ (10% and 12%, respectively), obtaining clear SEM images of these nanoparticles proved challenging. The scarcity of sub-100 nm particles made it difficult to isolate and identify them among the larger microscale structures visible in the images. The SEM images for various steps indicated that after removing all the impurities (hemicellulose, lignin, etc.), the diameter and size of pure cellulose had been greatly reduced, confirming the nanoscale measurements.

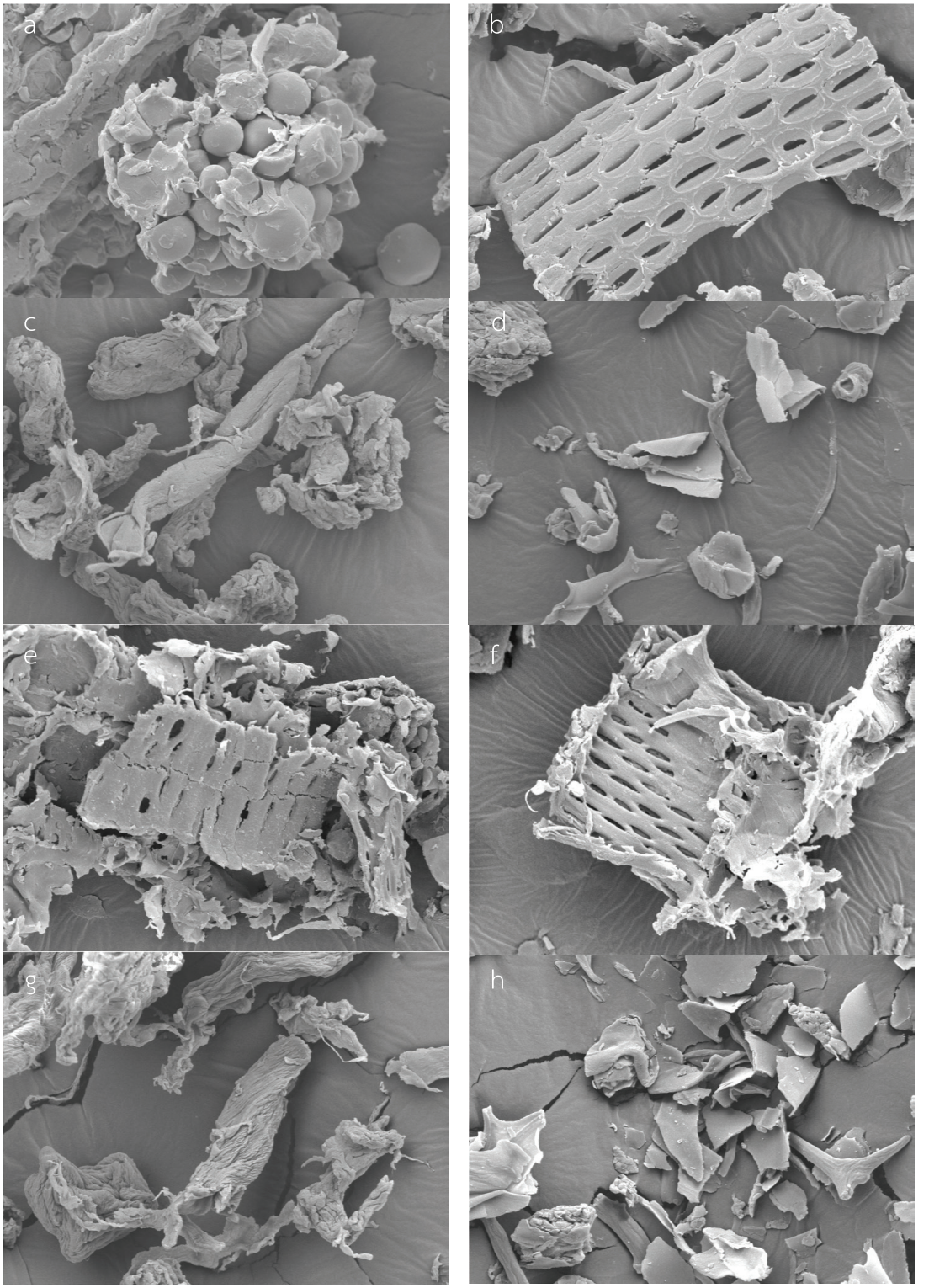

Figure 6 Scanning Electron Microscopy Images of a) CP; b) CP'; c) MCC'; d) NCC; e) CP_{biogas}; f) CP'_{biogas}; g) MCC_{biogas}; h) NCC_{biogas}

Mass Balance of NCC and NCC_{biogas}

Figures 7 and 8 show the mass balance of $NCC_{<100nm}$ and $NCC_{biogas<100nm}$ yields from CP and CP_{biogas} based on 100 g of dry CP and CP_{biogas} using H_2SO_4 hydrolysis. $NCC_{<100nm}$ and $NCC_{biogas<100nm}$ yields were 0.266 g and 0.539 g, respectively. This study highlights the potential of extracting cellulose from cassava pulp and biogas residues. This process offers a promising alternative for industrial applications.

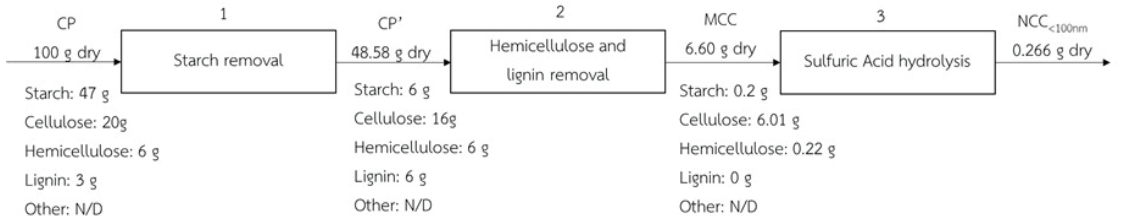

Figure 7 Mass Balance of $NCC_{<100nm}$ Yields from CP

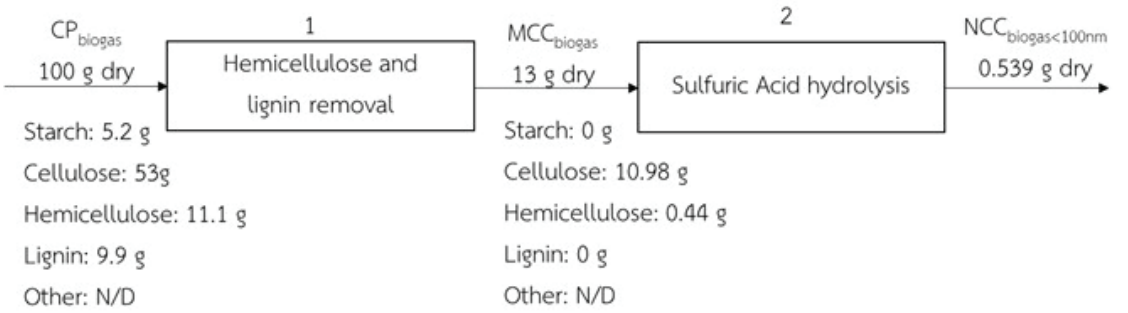

Figure 8 Mass Balance of $NCC_{biogas<100nm}$ Yields from CP_{biogas}

Conclusion

In summary, starch removal using **α**-amylase reduced the starch content of CP from 46.5% to 5.8% and completely removed the starch from CP_{biogas}. The bleaching process involving $NaClO_2$ and NaOH for CP and CP_{biogas} facilitated the production of a fibrous fraction with cellulose contents of 91% and 88%, respectively. MCC extracted from CP and CP_{biogas} had an average particle size ranging from 10-200 μm and a crystallinity index of 68% and 70%. After acid hydrolysis by H_2SO_4, the crystallinity index of NCC and NCC_{biogas} were increased to 71% and 76%, respectively with an average particle size ranging from 10-400 nm. The high CrI value achieved in this study renders the produced cellulose highly promising for innovative industrial applications, including the paper, composite, and textile industries.

The utilization of CP and CP_{biogas} enhances both economic value and sustainability within the cassava starch industry by converting these by-products into NCC. NCC has broad applications across multiple sectors, including packaging and pharmaceuticals. Furthermore, utilizing these byproducts reduces waste generated during starch production, promotes a circular economy approach, and consequently mitigates the environmental impact of the cassava industry. Ultimately, implementing strategies that enhance the value of byproducts and facilitate material recycling not only supports economic growth but also fosters long-term sustainability in the cassava starch industry.

Acknowledgments

The authors would like to acknowledge The Joint Graduate School of Energy and Environment (JGSEE), KMUTT, Thailand and the Center of Excellence on Energy Technology and Environment (CEE), Ministry of Higher Education, Science (MHESI), Research and Innovation for the financial support provided to perform this study with grant number JGSEE/THESIS/348, and the Excellent Center of Waste Utilization and Management (EcoWaste) for the equipment in the experiment and technical assistance.

References

1. Lerdlattaporn, R., Phalakornkule, C., Trakulvichean, S. and Songkasiri, W., 2021, "Implementing Circular Economy Concept by Converting Cassava Pulp and Wastewater to Biogas for Sustainable Production in Starch Industry," *Sustainable Environment Research*, 31 (1), pp. 1-12.
2. Sowcharoensuk, C., 2023, Industry Outlook 2023-2025: Cassava Industry [Online], Available: https://www.krungsri.com/en/research/industry/ industry-outlook/agriculture/ cassava/io/cassava-2023-2025#:~:text=Demand %20for% 20cassava%20will%20continue,of%20fresh%20cassava%20in%202023. [15 April 2023]
3. Trakulvichean, S., Chaiprasert, P., Otmakhova, J. and Songkasiri, W., 2019, "Integrated Economic and Environmental Assessment of Biogas and Bioethanol Production from Cassava Cellulosic Waste," *Waste and Biomass Valorization*, 10 (3), pp. 691-700.
4. Scarlat, N., Fahl, F., Dallemand, J.F., Monforti, F. and Motola, V., 2018, "A Spatial Analysis of Biogas Potential from Manure in Europe," *Renewable and Sustainable Energy Reviews*, 94, pp. 915-930.

5. Aziz, T., Farid, A., Haq, F., Kiran, M., Ullah, A., Zhang, K. and Al Jaouni, S.K., 2022, "A Review on the Modification of Cellulose and its Applications," *Polymers*, 14 (15), 34 p.
6. Reshamwala, S., Shawky, B.T. and Dale, B.E., 1995, "Ethanol Production from Enzymatic Hydrolysates of AFEX-treated Coastal Bermudagrass and Switchgrass," *Applied Biochemistry and Biotechnology*, 51, pp. 43-55.
7. Omran, A.A.B., Mohammed, A.A., Sapuan, S.M., Ilyas, R.A., Asyraf, M.R.M., Rahimian Koloor, S.S. and Petrů, M., 2021, "Micro-and Nanocellulose in Polymer Composite Materials: A Review," *Polymers*, 13 (2), p. 231.
8. Chen, X., Deng, X., Shen, W. and Jiang, L., 2012, "Controlled Enzymolysis Preparation of Nanocrystalline Cellulose from Pretreated Cotton Fibers," *BioResources*, 7 (3), pp. 4237-4248.
9. Chen, X.Q., Pang, G.X., Shen, W.H., Tong, X. and Jia, M.Y., 2019, "Preparation and Characterization of the Ribbon-like Cellulose Nanocrystals by the Cellulase Enzymolysis of Cotton Pulp Fibers," *Carbohydrate Polymers*, 207,pp. 713-719.
10. Zhang, Y., Lu, X.B., Gao, C., Lv, W.J. and Yao, J.M., 2012, "Preparation and Characterization of Nano Crystalline Cellulose from Bamboo Fibers by Controlled Cellulase Hydrolysis," *Journal of Fiber Bioengineering and Informatics*, 5 (3), pp. 263-271.
11. Spagnuolo, L., Beneventi, D., Dufresne, A. and Operamolla, A., 2024, "High Yield Synthesis of Cellulose Nanocrystals From Avicel by Mechano-Enzymatic Approach," *ChemistrySelect*, 9 (30), pp 1-7.
12. Wang, H., Xie, H., Du, H., Wang, X., Liu, W., Duan, Y., Zhang, X., Sun, L., Zhang X. and Si, C., 2020, "Highly Efficient Preparation of Functional and Thermostable Cellulose Nanocrystals Via H_2SO_4 Intensified Acetic Acid Hydrolysis," *Carbohydrate Polymers*, 239, 10 p.
13. Travalini, A.P., Prestes, E., Pinheiro, L.A. and Demiate, I.M., 2018, "Extraction and Characterization of Nanocrystalline Cellulose from Cassava Bagasse," *Journal of Polymers and the Environment*, 26, pp. 789-797.
14. Thiex, N.J., Manson, H., Anderson, S., Persson, J.Å. and Collaborators: Anderson, S., Bogren, E., Bolek, G., Budde, D., Ellis, C., Eriksson, S., Field, G., Frankenius, E., Henderson, C., Henry, C., Kapphahn, M., Lundberg, L., Manson, H., Moller, J., Russell, M., Sefert-Schwind, J. and Spann, M., 2002, "Determination of Crude Protein in Animal Feed, Forage, Grain, and Oilseeds by Using Block Digestion with a Copper Catalyst and Steam

Distillation Into Boric Acid: Collaborative Study," *Journal of AOAC International*, 85 (2), pp. 309-317.

15. Doehlert, D.C. and Duke, S.H., 1983, "Specific Determination of α-Amylase Activity in Crude Plant Extracts Containing β-Amylase," *Plant Physiology*, 71 (2), pp. 229-234.
16. Van Soest, P.V., Robertson, J.B. and Lewis, B.A., 1991, "Methods for Dietary Fiber, Neutral Detergent Fiber, and Nonstarch Polysaccharides in Relation to Animal Nutrition," *Journal of Dairy Science*, 74 (10), pp. 3583-3597.
17. Mandal, A. and Chakrabarty, D., 2011, "Isolation of Nanocellulose from Waste Sugarcane Bagasse (SCB) and Its Characterization," *Carbohydrate Polymers*, 86 (3), pp. 1291-1299.
18. Chen, Y., Liu, C., Chang, P.R., Cao, X. and Anderson, D.P., 2009, "Bionanocomposites Based on Pea Starch and Cellulose Nanowhiskers Hydrolyzed from Pea Hull Fibre: Effect of Hydrolysis Time," *Carbohydrate Polymers*, 76 (4), pp. 607-615.
19. Hu, H., Liang, W., Zhang, Y., Wu, S., Yang, Q., Wang, Y., Zhang, M. and Liu, Q., 2018, "Multipurpose Use of a Corncob Biomass for the Production of Polysaccharides and the Fabrication of a Biosorbent," *ACS Sustainable Chemistry & Engineering*, 6 (3), pp. 3830-3839.
20. Abraham, E., Deepa, B., Pothan, L.A., Jacob, M., Thomas, S., Cvelbar, U. and Anandjiwala, R., 2011, "Extraction of Nanocellulose Fibrils from Lignocellulosic Fibres: A Novel Approach," *Carbohydrate Polymers*, 86 (4), pp. 1468-1475.
21. Li, Q., Wei, B., Xue, Y., Wen, Y. and Li, J., 2016, "Improving the Physical Properties of Nano-cellulose Through Chemical Grafting for Potential Use in Enhancing Oil Recovery," *Journal of Bioresources and Bioproducts*, 1 (4), pp. 186-191.
22. Ouyang, X., Wang, W., Yuan, Q., Li, S., Zhang, Q. and Zhao, P., 2015, "Improvement of Lignin Yield and Purity from Corncob in the Presence of Steam Explosion and Liquid Hot Pressured Alcohol," *RSC advances*, 5 (76), pp. 61650-61656.
23. Ghazy, A., Bassuoni, M.T., Maguire, E. and O'Loan, M., 2016, "Properties of Fiber-Reinforced Mortars Incorporating Nano-silica," *Fibers*, 4 (1), pp. 1-16.